

tecting the nascent DNA from degradation, the amount of X-shaped intermediates is severely reduced in *recF* and *recR* mutants (Fig. 3C). Furthermore, although *recF* and *recR* mutants still fail to recover replication in the absence of either the RecQ helicase or the RecJ nuclease, the nascent DNA at the replication fork remains intact (10) and, in these mutants, the X-shaped intermediates are clearly restored (Fig. 3; fig. S2), indicating that a portion of the intermediates in the cone region are formed through the regression of the replication fork and the extrusion of the nascent DNA (Fig. 4). Thus, DNA lesions that block replication fork progression induce a regressed intermediate that is maintained by RecA and RecF, -O, and -R. In the absence of these proteins, the intermediate is degraded by RecQ and RecJ, which have been previously shown to process the nascent lagging strand before the resumption of replication (10). Recently, *rad53* checkpoint mutants in *Saccharomyces cerevisiae* have been shown to contain nascent lagging strand abnormalities and accumulate a similar intermediate after hydroxyurea treatment (24, 25), suggesting that similar mechanisms may operate in both prokaryotes and eukaryotes. It should be emphasized that not all lesions may block replication or be processed by the same mechanisms, and it is likely that a portion of the X-shaped intermediates in wild-type cells are produced through recombinational exchanges. This is especially true in the case of *uvrA* mutants in which multibranching molecules accumulate. It remains to be determined whether fork regression *in vivo* is promoted enzymatically or occurs spontaneously via positive supercoiling in front of the replication fork (26, 27). We propose that the regressed intermediate allows repair enzymes or alternative polymerases to gain access to the replication blocking lesions, thereby allowing processive replication to resume once the block to replication has been removed or bypassed. By analogy, the recovery of transcription has been shown to require the removal of the RNA polymerase and nascent transcript before repair enzymes can effect repair (28, 29). Consistent with this idea, the appearance and duration of the regressed replication fork intermediate coincides with the time it takes for the DNA lesions to be removed and robust replication to resume.

References and Notes

- R. B. Setlow, P. A. Swenson, W. L. Carrier, *Science* **142**, 1464 (1963).
- J. Courcelle, D. J. Crowley, P. C. Hanawalt, *J. Bacteriol.* **181**, 916 (1999).
- R. B. Setlow, W. L. Carrier, *Proc. Natl. Acad. Sci. U.S.A.* **51**, 226 (1963).
- W. D. Rupp, P. Howard-Flanders, *J. Mol. Biol.* **31**, 291 (1968).
- W. D. Rupp, C. E. I. Wilde, D. L. Reno, P. Howard-Flanders, *J. Mol. Biol.* **61**, 25 (1971).
- A. K. Ganesan, K. C. Smith, *Mol. Gen. Genet.* **113**, 285 (1971).

- A. K. Ganesan, *J. Mol. Biol.* **87**, 103 (1974).
- Z. Horii, A. J. Clark, *J. Mol. Biol.* **80**, 327 (1973).
- J. Courcelle, C. Carswell-Crumpton, P. C. Hanawalt, *Proc. Natl. Acad. Sci. U.S.A.* **94**, 3714 (1997).
- J. Courcelle, P. C. Hanawalt, *Mol. Gen. Genet.* **262**, 543 (1999).
- S. Rangarajan, R. Woodgate, M. F. Goodman, *Mol. Microbiol.* **43**, 617 (2002).
- Z. Horii, K. Suzuki, *Photochem. Photobiol.* **8**, 93 (1968).
- B. B. Konforti, R. W. Davis, *Proc. Natl. Acad. Sci. U.S.A.* **84**, 690 (1987).
- B. L. Webb, M. M. Cox, R. B. Inman, *Cell* **91**, 347 (1997).
- Q. Shan, J. M. Bork, B. L. Webb, R. B. Inman, M. M. Cox, *J. Mol. Biol.* **265**, 519 (1997).
- J. Courcelle, P. C. Hanawalt, *Proc. Natl. Acad. Sci. U.S.A.* **98**, 8196 (2001).
- J. K. Karow, L. Wu, I. D. Hickson, *Curr. Opin. Genet. Dev.* **10**, 32 (2000).
- K. Hanada *et al.*, *Proc. Natl. Acad. Sci. U.S.A.* **94**, 3860 (1997).
- K. L. Friedman, B. J. Brewer, *Methods Enzymol.* **262**, 613 (1995).
- L. Martin-Parras, P. Hernandez, M. L. Martinez-Robles, J. B. Schwartzman, *J. Mol. Biol.* **220**, 843 (1991).
- Materials and methods are available as supporting material on Science Online.
- K. Hanada, M. Iwasaki, S. Ihashi, H. Ikeda, *Proc. Natl. Acad. Sci. U.S.A.* **97**, 5989 (2000).
- T. Tsujimura, V. M. Maher, A. R. Godwin, R. M. Liskay, J. J. McCormick, *Proc. Natl. Acad. Sci. U.S.A.* **87**, 1566 (1990).
- M. Lopes *et al.*, *Nature* **412**, 557 (2001).
- J. M. Sogo, M. Lopes, M. Foiani, *Science* **297**, 599 (2002).
- P. McGlynn, A. A. Mahdi, R. G. Lloyd, *Nucleic Acids Res.* **28**, 2324 (2000).
- L. Postow *et al.*, *J. Biol. Chem.* **276**, 2790 (2001).
- I. Mellon, P. C. Hanawalt, *Nature* **342**, 95 (1989).
- C. P. Selby, A. Sancar, *Science* **260**, 53 (1993).
- We thank R. S. Lloyd for providing TEV, A. R. Poteete for providing bacterial strains, and D. J. Crowley and A. K. Ganesan for their comments. Supported by the National Science Foundation, grant MCB0130486.

Supporting Online Material

www.sciencemag.org/cgi/content/full/1081328/DC1
Materials and Methods

Figs. S1 and S2

References

9 December 2002; accepted 15 January 2003

Published online 23 January 2003;

10.1126/science.1081328

Include this information when citing this paper.

Taming of a Poison: Biosynthesis of the NiFe-Hydrogenase Cyanide Ligands

Stefanie Reissmann,¹ Elisabeth Hochleitner,² Haofan Wang,³ Athanasios Paschos,¹ Friedrich Lottspeich,² Richard S. Glass,³ August Böck^{1*}

NiFe-hydrogenases have an Ni-Fe site in which the iron has one CO and two CN groups as ligands. Synthesis of the CN ligands requires the activity of two hydrogenase maturation proteins: HypF and HypE. HypF is a carbamoyl-transferase that transfers the carbamoyl moiety of carbamoyladenylate to the COOH-terminal cysteine of HypE and thus forms an enzyme-thiocarbamate. HypE dehydrates the S-carbamoyl moiety in an adenosine triphosphate-dependent process to yield the enzyme thiocyanate. Chemical model reactions corroborate the feasibility of this unprecedented biosynthetic route and show that thiocyanates can donate CN to iron. This finding underscores a striking parallel between biochemistry and organometallic chemistry in the formation of an iron-cyano complex.

Hydrogenases catalyze the reversible oxidation of molecular hydrogen into protons and electrons. They are widely distributed among microorganisms, and they provide them with the capacity either to use hydrogen as an energy source or to dissipate excess reducing equivalents in the form of molecular hydrogen. These enzymes have attracted considerable attention, not only

because of the distinctive chemical nature of their substrate and the reaction mechanism but also because of their potential biotechnological applications (1).

Two major classes of hydrogenases can be differentiated according to the metal content of the active site cofactor: Fe-hydrogenases and NiFe-hydrogenases. Although the overall structure of their metal centers differs, they share one unusual feature: diatomic, nonproteinaceous iron ligands, namely, carbon monoxide and cyanide. In NiFe-hydrogenases, the iron of the center carries two cyanide and one carbon monoxide moieties (2). The presence of these ligands stabilizes iron in a low oxidation and spin state.

In metal center synthesis and incorporation into proteins, important issues are con-

¹Department Biologie I, Mikrobiologie, University of Munich, Maria-Ward-Strasse 1a, D-80638 Munich, Germany. ²Max-Planck Institut für Biochemie, Abteilung Proteinchemie, Am Klopferspitz, D-82152 Martinsried, Germany. ³Department of Chemistry, University of Arizona, Post Office Box 210041, Tucson, AZ 85721-0041, USA.

*To whom correspondence should be addressed. E-mail: august.boeck@lrz.uni-muenchen.de

REPORTS

tol of the fidelity of insertion of the correct metal into the cognate target protein, maintenance of a folding state of the protein competent for metal addition, and conformational change to internalize the assembled metal center (3). In this context, the synthesis of the CN and CO ligands of NiFe-hydrogenases poses intriguing questions because of their

toxicity in the free state and, in particular, because addition of CO and CN to the metal reflects organometallic chemistry unprecedented in biology.

A total of seven auxiliary proteins are required for the synthesis and incorporation of the metal center in NiFe-hydrogenases (4). One of them, the HypF protein, accepts car-

bamoyl phosphate (CP) as a substrate and catalyzes both a CP phosphatase reaction in the absence of any other substrate and a CP-dependent hydrolysis of ATP into AMP and inorganic pyrophosphate (PP_i). Because the latter reaction is reversible, as shown by a CP-dependent pyrophosphate-ATP exchange, it was postulated that an adenylated CP derivative is an intermediate in the reaction and that the CP phosphatase activity may reflect a side reaction followed in the absence of ATP (5). The necessity of CP for the synthesis of the metal center was then clearly proven by the inability of mutants devoid of CP synthetase activity to mature NiFe-hydrogenases (6).

The formation of an adenylated CP derivative by HypF prompted studies on catalytic self-carbamoylation of the protein. To determine whether a stable carbamoyl derivative of purified HypF protein from *Escherichia coli* is formed, a filter binding assay was devised (7) (Fig. 1). The radioactivity of ¹⁴C-labeled CP was not stably incorporated into the HypF protein per se (Fig. 1A, second bar). HypF and HypE from *Helicobacter pylori* reportedly interact with each other (8), and HypE shares sequence similarity with the PurM protein, which catalyzes an ATP-dependent dehydration reaction during purine biosynthesis (9), a reaction that formally could also transform a carbamoyl into a cyano moiety. Consequently, transcarbamoylation of HypE catalyzed by HypF was studied. Purified HypE protein from *E. coli* indeed was found to hydrolyze ATP into ADP and inorganic phosphate in the absence of any other substrate (10). When HypE was incubated with the HypF protein from the same organism with different molar ratios in the presence of ATP and CP (Fig. 1A), a stable adduct between radiolabeled CP and the HypE protein was formed. Its radioactivity quantitatively correlated with the amount of HypE, but not HypF, protein used in the assay. The stoichiometry between CP-derived radioactivity and HypE protein was between 50 and 60%. These results support the conclusion that HypF is required for the transfer of the carbamoyl group of CP to HypE. This transfer depends on the cleavage of ATP into AMP and PP_i (Fig. 1B). With the nonhydrolyzable analog ADP-CH₂-P (in which a methylene group replaces the phosphoanhydride bond) in place of ATP, transfer still took place, but in the presence of AMP-CH₂-PP, it was blocked. These results are consistent with HypF functioning as a carbamoyltransferase that requires prior adenylation of CP, which is not possible with AMP-CH₂-PP as a substrate.

To prove that the HypE protein indeed acts as the acceptor and to study whether binding of the putative carbamoyl residue is covalent, HypE and HypF were incubated

Fig. 1. Modification of the hydrogenase maturation protein HypE by the HypF protein. (A) Binding of radioactively labeled CP to HypF and/or HypE proteins assessed by binding of the proteins to nitrocellulose filters. HypEΔC is a HypE variant lacking the COOH-terminal cysteine residue. (B) HypE (2 μM) and HypF (2 μM) were reacted with radioactive CP in the absence of ATP (bar 1), in the presence of ADP-CH₂-P (bar 2) or AMP-CH₂-PP (bar 3). Bar 4 presents the result of a standard assay with ATP as substrate, but the assays contained 250 μg bovine serum albumin instead of HypE and HypF. (C and D) Lane 1 contains only HypF; lane 2 contains only HypE. (Lanes 3 to 6): HypF protein (2 μM) was reacted with 6 μM HypE protein in the assay mixture given above, which contained as nucleoside triphosphate (NTP) (a) ATP, (b) AMP-CH₂-PP, or (c) ADP-CH₂-P. On the right, F in (C) denotes HypF; E indicates HypE, and E*, a dimer of HypE. Denaturation with SDS in the absence of dithiothreitol (DTT) allows more radioactivity to be recovered, which indicates that the adduct is labile to thiols. The altered migration possibly reflects an oxidized form of HypE.

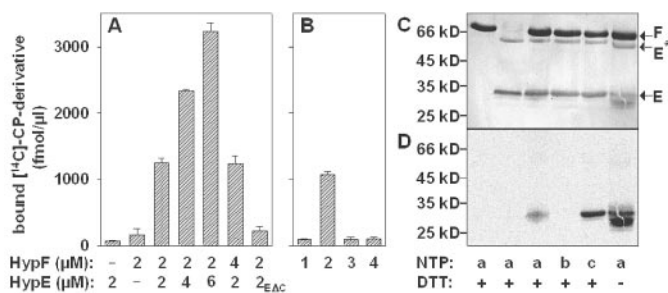
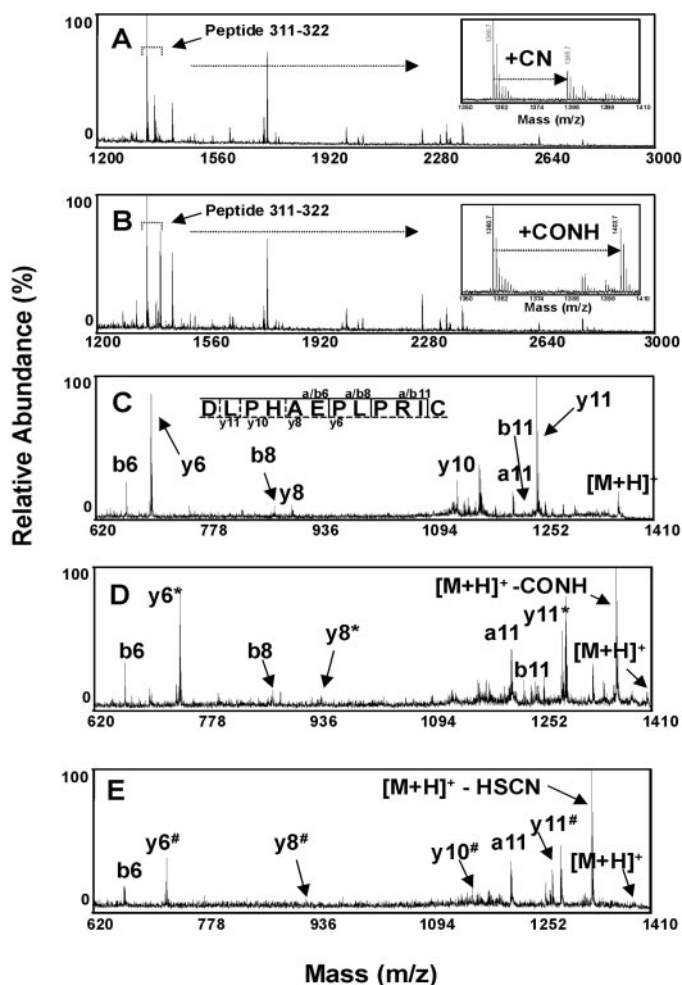


Fig. 2. Mass and tandem mass spectrometric analysis of HypE protein modified by HypF. (A) Spectrum of a reaction of HypE, HypF, CP, and ATP and (B) like (A) but with ADP-CH₂-P instead of ATP, digested with endoproteinase Asp-N. Peptide 311-322 (m/z 1360.7) modified with (A) CN (m/z 1385.7) and (B) CONH₂ (m/z 1403.7) is enlarged. (C) depicts the tandem mass spectrum of unmodified peptide 311-322 (m/z 1360.7), (D) of peptide 311-322 modified with CONH₂ (m/z 1403.7), and (E) of the peptide modified with CN (m/z 1385.7). y ions modified with CONH₂ and CN are labeled with (*) and (#), respectively. For clarity, only the spectrum of the m/z range from 640 to 1500 is depicted. The peptide designation follows the standard nomenclature (22) [for details see the insert in Fig. 2C and (7)].



with [^{14}C]CP and ATP, and then the assay mixture was denatured by SDS under reducing and nonreducing conditions, separated by SDS-polyacrylamide gel electrophoresis (SDS-PAGE), and blotted onto a nitrocellulose membrane. The blot was autoradiographed (Fig. 1D) and then stained (Fig. 1C) (7). The results show that the radioactivity is transferred to HypE during the reaction and that the binding is stable under denaturing conditions, which suggests covalent attachment.

Apart from the sequence similarity with the PurM protein, HypE carries a PRIC motif as the last four amino acids (Pro-Arg-Ile-Cys), which is invariable in all members of the HypE family. This cysteine residue at the COOH-terminus prompted speculation that its thiol group might be the target for carbamoylation. Indeed, the purified HypE variant with a deletion of this amino acid could not accept the putative carbamoyl group transferred by HypF (Fig. 1A, last bar).

To identify the amino acid residue of HypE that is modified, samples of the reaction mixtures were digested with endoproteinase Asp-N, and the peptides were analyzed by mass spectrometry (Fig. 2) (7). The peptide pattern of an assay containing HypF, HypE, and CP plus ATP differed from that of a control assay lacking CP (11) in the appearance of a single peptide with a mass of 1385.7. This peptide corresponds to the COOH-terminal peptide of the HypE protein, ranging from amino acid 311 to 322 (mass 1360.7), and the mass of the additional peptide is compatible with the presence of a cyano group replacing a hydrogen from an amino acid side chain (Fig. 2A).

Because HypE has intrinsic adenosine triphosphatase activity and exhibits sequence similarity to PurM, an enzyme catalyzing an ATP-dependent dehydration reaction, it seemed feasible that the CN modification derives from the dehydration of a carbamoyl precursor. This conjecture was tested by analyzing the peptide pattern of an assay in which ATP was replaced by the nonhydrolyzable ADP- $\text{CH}_2\text{-P}$. Under this condition, the transcarbamoylation by HypF (requiring cleavage of ATP into AMP and PP_i) should still be possible, but the dehydration should be blocked. The mass increment of peptide 311-322 increases from 1360.7 to 1403.7 (Fig. 2B); this proves that HypE indeed carries a carbamoyl modification. To identify the amino acid residue carrying the carbamoyl or the cyano modification, tandem mass spectrometry (MS/MS) of this peptide from assays lacking CP and ATP (Fig. 2C) was performed. The pattern was compared with those from reactions delivering carbamoylated (in the presence of CP and ADP- $\text{CH}_2\text{-P}$) (Fig. 2D) or cyanated (in the presence of CP and ATP) (Fig. 2E) HypE protein. It

was found that, in the MS/MS spectrum of the 311-322 peptide derived from a reaction in which the substrates were present, all y ions but no b ions carried the modification (Fig. 2, D and E). Moreover, one peptide, a11/b11, corresponds to a fragment of amino acids 311 to 321 (lacking the cysteine). Because it also lacks the modification, it is clear that each of the modifications is bound to the COOH-terminal cysteine. Finally, the spectrum shown in Fig. 2E demonstrates that HSCN is cleaved off the precursor; therefore, it is the COOH-terminal cysteine that is either cyanated or carbamoylated.

The steps in CN formation catalyzed by the hydrogenase maturation proteins HypF and HypE are summarized in Fig. 3. HypF forms the postulated AMPOCONH $_2$ from which the carbamoyl group is transferred to the COOH-terminal cysteine of HypE (step 1). HypE-carbamoylation (step 1) is followed by the ATP-dependent dehydration by HypE (step 2) and the transfer to the iron atom (step 3).

Chemical models were studied to determine the chemical feasibility of steps 2 and 3 in Fig. 3 and related reactions. The reactions carried out are shown in Fig. 4 (7). Thus,

Fig. 3. Biosynthesis of the cyanide ligand. (Step 1), formation of carbamoyladenylate by HypF (F) as delineated from the ATP- PP_i exchange reaction, and carbamoyl transfer to the COOH-terminal cysteine of HypE (E). (Step 2), ATP-dependent dehydration involving phosphorylation of the carbonyl oxygen of CP followed by dephosphorylation. (Step 3), chemical transfer of the cyano group to iron.

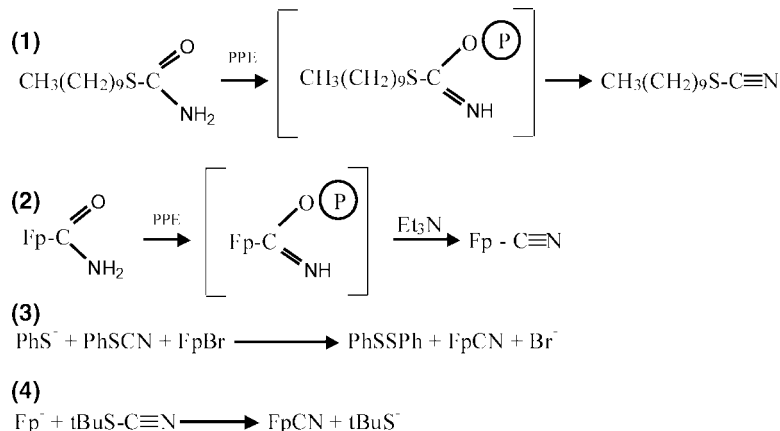
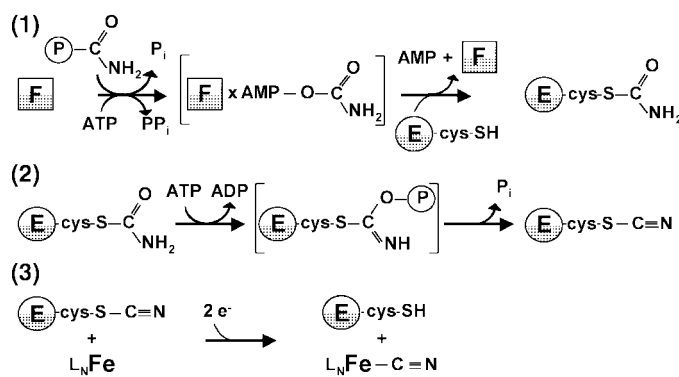


Fig. 4. Chemical models for the proposed biosynthesis of L_nFeCN . (1) Dehydration of *S*-(*n*-decyl) thiocarbamate to the corresponding thiocyanate with ethyl polyphosphate (PPE). (2) Dehydration of iron carboxamido complex to iron cyanide where Fp is $(\eta^5\text{-C}_5\text{H}_5)\text{Fe}(\text{CO})_2$. (3) Transfer of a nucleophilic CN group to electrophilic iron atom. (4) Transfer of an electrophilic CN group to nucleophilic iron atom.

philic. Treating *t*-butylthiocyanate with Fp⁻ brought about a 20% yield of FpCN (17) [Fig. 4 (reaction 4)]. These chemical models validate the feasibility of the proposed biosynthesis of the CN ligand and its transfer from sulfur to iron (18).

In sum, the cysteine residue of HypE undergoes unprecedented biotransformations in serving as the site for dehydration of a carboxamido moiety to CN, in carrying the CN residue, and in transferring the CN to iron. Previously, thiocyanates were rarely encountered in nature. Thiocyanate synthesis in the marine sponge *Axinyssa n. sp.* has been proposed to involve sulfuration of cyanide to give ⁻SCN followed by reaction with a sesquiterpene cation (19), although cyanation of a thiol moiety has also been suggested (20, 21).

References and Notes

- P. M. Vignais, B. Billoud, J. Meyer, *FEMS Microbiol. Rev.* **25**, 455 (2001).
- M. Frey, J. C. Fontecilla-Camps, A. Volbeda, in *Handbook of Metalloproteins*, A. Messerschmidt, R. Huber, K. Wieghardt, T. Poulos, Eds. (Wiley, New York, 2001), pp. 880–896.
- R. P. Hausinger, in *Mechanisms of Metallocenter Assembly*, R. P. Hausinger, G. L. Eichhorn, L. G. Marzilli, Eds. (Wiley-VCH, New York, 1996), pp. 1–18.
- M. Blokesch et al., *Biochem. Soc. Trans.* **30**, 674 (2002).
- A. Paschos, A. Bauer, A. Zimmermann, E. Zehelein, A. Böck, *J. Biol. Chem.* **277**, 49945 (2002).
- A. Paschos, R. S. Glass, A. Böck, *FEBS Lett.* **488**, 9 (2001).
- Materials and methods are available as supporting material on Science Online.
- J. C. Rain et al., *Nature* **409**, 211 (2001).
- C. Li, T. J. Kappock, J. Stubbe, T. M. Weaver, S. E. Ealick, *Structure Fold Des.* **7**, 1155 (1999).
- A. Paschos, S. Reissmann, A. Böck, unpublished data.
- E. Hochleitner, S. Reissmann, F. Lottspeich, A. Böck, unpublished observations.
- G. Burkhardt, M. P. Klein, M. Calvin, *J. Am. Chem. Soc.* **87**, 591 (1965).
- J. R. Van Wazer, S. Norval, *J. Am. Chem. Soc.* **88**, 4415 (1996).
- Dehydration of citrullines to cyanamides with *p*-toluenesulfonyl chloride and pyridine, i.e., RNHCONH₂ → RNHCN, was reported in a chemical simulation of arginine biosynthesis and the urea cycle (23).
- For evidence supporting the relevancy of modeling the active site of [NiFe] hydrogenase with Fp complexes, see (24).
- A. Jungbauer, H. Behrens, *J. Organomet. Chem.* **186**, 361 (1980).
- Although this reaction may involve nucleophilic displacement by iron of thiolate at the cyano carbon atom, an electron transfer mechanism is also possible.
- There are two possibilities for the origin of the CO ligands: hydrolysis of a CN ligand and transfer of a carbamoyl group to iron followed by deamination. Hydrolysis of a CN ligand is analogous to the known hydrolysis of iron isocyanides to iron carbonyl complexes (25). Deamination of carboxamido iron complexes is also known (26).
- J. S. Simpson, M. J. Garson, *Tetrahedron Lett.* **39**, 5819 (1998).
- A. T. Pham et al., *Tetrahedron Lett.* **32**, 4843 (1991).
- C. Jimenez, P. Crews, *Tetrahedron* **47**, 2097 (1991).
- P. Roesdörff, J. Fohlman, *Biomed. Mass Spectrom.* **11**, 601 (1984).
- D. Ranganathan, R. Rathi, *J. Org. Chem.* **55**, 2351 (1990).
- C.-H. Lai et al., *J. Am. Chem. Soc.* **120**, 10103 (1998).
- V. Riera, J. Ruiz, *J. Organomet. Chem.* **384**, 339 (1990).
- L. Busetto, R. J. Angelici, *Inorg. Chim. Acta* **2**, 391 (1968).

27. We thank the Deutsche Forschungsgemeinschaft and the Fonds der Chemischen Industrie for supporting the research of A.B. and the donors of the Petroleum Research Fund, administered by American Chemical Society, for support of this research (ACS-PRF 37202-AC3, R.S.G. and H.W.).

Supporting Online Material

www.sciencemag.org/cgi/content/full/299/5609/1067/DC1
Materials and Methods
References and Notes

2 December 2002; accepted 15 January 2003

Single-Neuron Activity and Tissue Oxygenation in the Cerebral Cortex

Jeffrey K. Thompson, Matthew R. Peterson, Ralph D. Freeman*

Blood oxygen level–dependent functional magnetic resonance imaging uses alterations in brain hemodynamics to infer changes in neural activity. Are these hemodynamic changes regulated at a spatial scale capable of resolving functional columns within the cerebral cortex? To address this question, we made simultaneous measurements of tissue oxygenation and single-cell neural activity within the visual cortex. Results showed that increases in neuronal spike rate were accompanied by immediate decreases in tissue oxygenation. We used this decrease in tissue oxygenation to predict the orientation selectivity and ocular dominance of neighboring neurons. Our results establish a coupling between neural activity and oxidative metabolism and suggest that high-resolution functional magnetic resonance imaging may be used to localize neural activity at a columnar level.

Functional magnetic resonance imaging (fMRI) is a powerful tool used for the non-invasive mapping of neural activity in the brain (1–3). Blood oxygen level–dependent (BOLD) fMRI infers neural activity by measuring small changes in deoxyhemoglobin within the brain's vasculature. Therefore, the coupling between local cerebral hemodynamics and the underlying neural activity is critically important to the interpretation and design of fMRI studies. Increases in neural activity elicit a delayed decrease in deoxyhemoglobin corresponding to a positive change in the BOLD signal (1–4). Most fMRI investigations use this positive BOLD response to map neural activity. However, because the response is also observed from draining veins that are displaced from the sites of activation, the spatial resolution is limited (5–7). Optical imaging and imaging spectroscopy findings suggest that a fast increase in deoxyhemoglobin, occurring before the delayed decrease, may be a better indicator of neural activity (8, 9). This component of the hemodynamic response is often referred to as the “initial dip.” Recent fMRI studies and direct measurements of oxygen tension within the microcirculation have also identified the initial dip (6, 7, 10–12). In studies of the visual cortex, brain imaging maps that emphasize the initial

dip exhibit sharper patches and stripes [characteristic of orientation and ocular dominance columns (13)] relative to functional maps that are based on other signals (6, 8, 9). It has been proposed that the initial dip reflects an increase in oxygen consumption by active cells and is consequently better localized to the site of neural activity (6, 8, 9).

Despite its potential, the existence and interpretation of the initial dip are controversial because it is not always observed using fMRI (14, 15), and its detection using imaging spectroscopy may be confounded by the difficulty in correcting for the wavelength dependence of light scattering in tissue (16, 17). An alternative hypothesis is that changes in blood volume, rather than oxygen consumption, could account for the initial dip (18). Although simultaneous recordings of fMRI signals and neural activity were recently reported in the monkey's primary visual cortex (4), the analysis focused on the positive BOLD response and used stimuli that were designed to activate a relatively large uniform area of the cortex. Therefore, the studies did not address neural and hemodynamic coupling at a submillimeter spatial resolution.

In our study, we made simultaneous colocalized measurements of tissue oxygenation and single-cell neural activity in area 17 of the cat's visual cortex. Tissue oxygenation is linked to deoxyhemoglobin through the local oxygen concentration gradient in tissue and through the oxygen-hemoglobin dissociation curve and is therefore expected to reflect the hemodynamic changes measured with fMRI. A quantitative model of cerebral hemody-

Group in Vision Science, School of Optometry, Helen Willis Neuroscience Institute, University of California, Berkeley, CA 94720–2020, USA.

*To whom correspondence should be addressed. E-mail: freeman@neurovision.berkeley.edu